17

Monitoring Preparation of Derivative Protein Crystals *via* Raman Microscopy

Antonello Merlino, Filomena Sica and Alessandro Vergara*
Department of Chemistry, University of Naples "Federico II", Naples, Italy Istituto di Biostrutture e Bioimmagini, CNR, Naples Italy

1. Introduction

Below to crystallographic applications, protein crystals are of great interest in other numerous fields of biology and biotechnology. Cataract, or the loss of transparency of the eye lens, is related to the alteration of physical, chemical, and structural properties of proteins of the crystallin family, that may lead to crystallization under some physiological conditions (Tardieu, 1998). Other pathological states are known to be a consequence of the *in vivo* formation of crystals, made of either proteins or other macromolecular assemblies. Examples are viral proteins stored in plant cells, viral particles in animal cells, hemoglobin C and S causing anemia, or ribosomal particles accumulating in the brain of patients suffering from *presenile dementia* (McPherson, 1999).

Of course, crystals of biological macromolecules that are prepared *in vitro* have important applications: they are tools to obtain atomic models of the molecules and to design specific ligands and new drug formulations. Medicinal formulations composed of either insulin (Richards et al., 1999) or α-interferon crystals (Reichert et al., 1996) are already applied in treatments to ensure the continuous release of protein in blood. Crystallographic analysis of highly ordered crystals with intense X-ray sources provides accurate three dimensional structures (Ducruix & Giegé, 1999). The success of this technique strictly depends on obtaining diffraction-quality crystals. The process of crystallization remains a hit-and-miss affair, typically involving screening hundreds of conditions. The crystallization of biological macromolecules shares many common properties with those of small solute molecules (e.g. growth by 2D nucleation or by screw dislocation mechanisms), but their crystals exhibit several peculiarities: most of them have a high solvent content (e.g. 30-80 vol%), few intermolecular contacts, and a high density of defects (Malkin et al., 1996).

Briefly, protein crystallization requires the formation of a supersaturated protein-precipitant solution. The transition from a stable solution to a supersaturated one can be achieved by increasing the concentration of precipitant and/or that of protein (Vergara et al., 2003). The most frequently used crystallization method is the *vapor diffusion technique*. A drop containing protein, buffer, salt and precipitant is equilibrated against a reservoir (buffer, salt and precipitant). The difference in concentration between the drop (lower) and the reservoir (higher) drives the system toward equilibrium by diffusion through the vapor phase. The drop can either be placed on the underside of the cover slide (*hanging drop*) or placed on a

plastic support above the surface of the reservoir (*sitting drop*). *Batch crystallization* is a method where the sample is mixed with precipitant and additives creating a homogenous crystallization medium. In the *free interface diffusion* the protein sample is stratified over the precipitant solution; over time the sample and precipitant diffuse into one another and crystallization may occur at the interface. In a *microdialysis experiment* the protein solution is equilibrated through a membrane against the precipitant solution over time in a stepwise manner. In some cases, to improve the X-ray diffraction properties the crystallization is performed in a gel medium. Agarose, agar and silica have been successfully used as gel materials to obtain protein crystals (Chayen, 1998; Vergara et al., 2003; Vergara et al., 2009).
It is a frequent task to produce modified protein crystals in order to study the structural modifications undergoing a chemical treatment. These derivative crystals can be prepared *via* co-crystallization, or *via* soaking. Co-crystallization means that crystallization of the chemically modified biopolymers (protein and additive) is conducted from solution phase. Alternatively, protein crystals are first grown and then they are chemically modified *via* diffusion of the additives that are soaked into the solvent channels. Both these preparative procedures can be supported by the application of Raman monitoring, particularly by difference Raman spectra (in co-crystallization) or by a time-resolved Raman microscopy (for soaking procedure).

2. Principles of Raman spectroscopy

2.1 Raman effect

Raman spectroscopy is a vibrational spectroscopy based on the anelastic scattering of a monochromatic light (frequency ν) due to the interaction with the sample. The polarizability tensor of the sample oscillating with a normal frequency ν_0, that is associated to the *omni* present molecular vibrations, interacts with the electric field of the laser light. This produces an induced electric dipole oscillating (then irradiating) with three distinct frequency (ν, $\nu+\nu_0$ and $\nu-\nu_0$). The strong elastic scattering at frequency ν_0 is the Rayleigh scattering that usually is cut in a Raman experiment. The two minor inelastic components are Raman Stokes bands ($\nu-\nu_0$) and Raman antiStokes ($\nu+\nu_0$). At room temperature only Raman stokes bands are intense enough to be recorded. The difference between the wavenumber of the incident light and the scattered Raman band is the *Raman shift* (the x-axis of any Raman spectrum). The y-axis is usually reported in arbitrary units, so that accurate quantitative analysis can be based only on ratio of two distinct bands or by using some internal standard. In the Stokes Raman region (at wavelength lower than the excitation line) also fluorescence is collected. Therefore the counts read in the y-axis is always the sum of Raman and fluorescence, that should be kept as low as possible.

2.2 Off-resonance and resonance Raman

We should point out that two major kinds of Raman spectra can be collected, depending on the laser line (off-resonant Raman and resonant Raman spectra). In off-resonance Raman spectra no relation exists between excitation line and electronic absorption condition. On the contrary, resonance Raman spectra are collected when a particular excitation wavelength is used, namely within one electronic absorption band of the sample. Resonance Raman spectra are much more intense (depending on the extinction coefficients of the electronic transition) and selective (only normal mode that couples with the vibronic transition can be

enhanced) than off-resonance Raman spectra. A more extensive presentation of the quantum mechanics of the Raman effect is elsewhere reported (Long, 2002).

3. Handling of protein crystals for Raman microscopy experiments

Raman microscopy is ideal for the monitoring of bioprocesses as it is non-destructive, inexpensive, rapid and quantitative. Its confocal nature makes it possible to focus through transparent capillary or directly on crystals kept in their crystallization reactor allowing straight analysis on the sample.
In co-crystallization experiments two independent Raman spectra are collected on native and derivative crystals, using the same mother liquor with the exception of the reactant. In this case, the comparative analysis of the two spectra can provide differences in a) number, b) position and c) intensity of protein Raman bands. Manipulation of crystals for Raman measurements requires standard handling.

3.1 Crystal sampling

Confocal apparatus allows to get rid of any influence of the cover slip (as in vapour diffusion) or container wells (as in FID or batch crystallization supports). Measurement into drops (both hanging and sitting drop) is particularly feasible. In order to avoid significant scattering from mother liquor, thus reduction in spectral quality, it is better to keep the drop as small as possible, and to use a minimal depth into the crystal (particularly for resonance Raman spectra). Water is a weak Raman scatterer, with a small contribution at 1640 cm^{-1}. Precipitating agents, especially when at high content (PEG, MPD, alcohol) may interfere or not, depending on the spectral region of interest. Agarose and silica gel matrix do not interfere significantly, so crystals grown in gel medium can be used as well.
Despite we deal with solid state we will not consider frequencies of the lattice vibrational modes, that for protein crystals are very low (below the Rayleigh cut). For lysozyme crystals it is 25 cm^{-1}.
We will focus on two distinct experimental setups, namely for *in-situ* and *ex-situ* Raman spectroscopy, referred to simultaneous or not to X-ray diffraction experiments (also reported as on-line and off-line (McGeehan et al, 2011)). Below we present separately these two setups and applications.

3.2 Ex situ Raman experiments

Most of the analysis to monitor chemical modification of protein crystals can be performed by *ex situ* Raman experiments, which involve distinct acquisition of Raman and X-ray diffraction data. The experiments are, indeed, carried out on a Raman microscope that is physically separated from the X-ray diffractometer. This kind of experiments can be easily performed on a commercial or home-built Raman microscope, and it aims to the definition of the experimental conditions (eg soaking time and reactant/protein molar ratio) for the preparation of derivative protein crystals. Raman spectra on very small drops can be recorded also at low temperatures by using a dedicated autostage (Linkham Co), though care must be taken during cooling to ensure high transparency of the drop and to avoid crystal movement within the drop. When flash freezing is adopted, these impediments are overcome. Crystals monitored at room temperature *via* ex situ apparatus can even be frozen and taken to the X-ray diffractometer for the data collection.

3.3 Raman microscopy apparatus

The Raman confocal microscope (Jasco, NRS-3100) currently available for *ex-situ* experiments at the Department of Chemistry of the University of Naples 'Federico II' is depicted in Figure 1. One of the 458, 488 and 514-nm lines of an air-cooled Ar^+ laser (Melles Griot, 35 LAP 431-220), or 406, 413 and 647 nm lines of a water-cooled Kr^+ laser (Coherent, Innova 320) can be injected into an integrated Olympus confocal microscope and focused to a spot size of approximately 2 μm by a 100x or 20x objective. The laser power at the sample depends on the wavelength ranging from 5 to 100 mW. A holographic notch filter is used to reject the excitation laser line. Raman back-scattering is dispersed through a monochromator (2400 or 1200 grooves/mm grating) and collected by a Peltier-cooled 1024 x 128 pixel CCD photon detector (Andor DU401BVI). Frequency shifts are calibrated by using indene, cyclohexane or CCl_4 as standard, depending on the spectral range of interest. An acceptable spectral resolution is usually considered 4 cm^{-1}.

Actually, since Raman shift for off-resonant spectra is independent of the excitation wavelength, in principle also IR or UV excitation could be used, though at least different optics and detector (a different apparatus) is required.

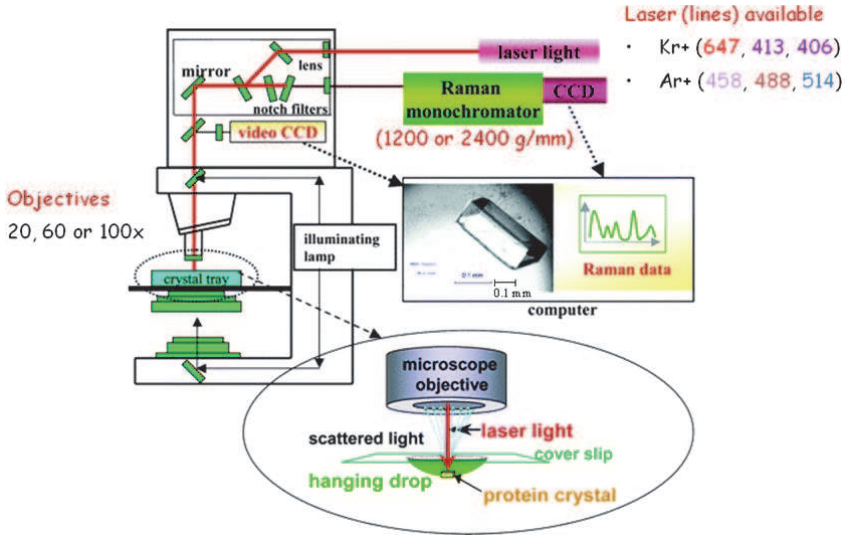

Fig. 1. Scheme of Raman apparatus available at the University of Naples "Ferderico II" (Dept of Chemistry) to collect spectra from protein single crystals. Adapted after (Carey & Dong, 2004).

3.4 In situ Raman experiments

Whether the crystal is on the diffractometer or away from it (*in situ* or *ex situ*), Raman spectra are not affected by it, but of course only *in-situ* analysis reveals radiation damage effects (that could be even reversible (Adam et al, 2009)).

That is the reason for many efforts in the last decades to make Raman microscopes available at synchrotron beamlines: the European Synchrotron Radiation Facility (ESRF) (Carpentier et al. 2007), National Synchrotron Light Source (NSLS), Brookhaven National Laboratory (BNL) (Stoner-Ma et al., 2011) and Swiss Light source (SLS) (Owen et al. 2010) part-time

dedicates one of their beamlines to *in situ* Raman-assisted X-ray biocrystallography (see below).

A recent review on the microRaman apparatus available at synchrotron facility is reported in (McGeehan et al., 2011). For *in situ* setup we intend that the X-ray diffractometer is integrated with a laser (guided by an optical fiber) that is backscattered to a spectrograph. To this end, crystals are mounted on an usual crystallographic head kept into a cryo-loop under a nitrogen flux (typically at 100 K). After the crystal is centered for X-ray diffraction data collection experiments, the optimal orientation for the collection of the best Raman spectra has to be determined, typically by manually re-orienting the crystal. Once the crystal orientation that results in the best signal-to-noise ratio is found, Raman spectra are acquired prior and after the X-ray diffraction data collection, at the same crystal orientation. This allow to check if any photo-chemistry is induced by the X-ray beam exposure. For off-resonance Raman spectra it is particularly important to keep the drop volume low and to avoid interference from the loop (nylon loops should not intersect the Raman laser beam path (Carpentier et al., 2011)). When Raman spectra are collected as a function of the crystal orientation (Raman crystallography), information can be obtained on the orientation order and the variability of the relative intensity of Raman bands can be estimated (Tsuboi et al., 2007). Indeed, both off-resonance (Kudryavtsev et al., 1998) and resonance spectra (Smulevich & Spiro 1990) are mildly affected by crystal orientation. In this case general physical chemistry rather than structural information can be extracted by Raman crystallography.

4. Interpretation of Raman spectra of derivative protein crystals

4.1 Raman spectra analysis

A Raman spectrum provides a lot of information: energy shift, intensity and polarization of the scattered light and width of the peak. We will mostly focus on the Raman shift and intensity features. Each Raman shift corresponds to a permitted vibrational transition that relates to the strength constant k of the harmonic oscillator *via*

$$\nu = \frac{1}{2\pi}\sqrt{\frac{k}{\mu}} \tag{1}$$

where μ is the reduced mass. Therefore high frequency corresponds to either stretching or bending with a high strength constant or involving light atoms, such as hydrogen. The presence of the reduced mass at the denominator in equation 1 justifies the wide use of isotopic replacement (eg H/D) for band assignment. Raman transition corresponds, most likely, to a fundamental transition (from the vibrational ground state to the first excited state). Indeed, overtone and combination bands in Raman spectroscopy are much more unlikely than in Infrared spectroscopy (FT-IR). Furthermore, compared to FT-IR, Raman spectroscopy has very different selection rules, and usually bands that are strong in the IR absorption, are not allowed in Raman scattering. Indeed, the great advantage of Raman when studying biological samples is the very weak contribution from water to Raman spectra, compared to IR spectra.

Once Raman spectrum has been recorded, reduction for the temperature correction can be performed (Pernice et al., in press). Unless strictly necessary, as for a variable fluorescence coming from background, no baseline correction should be performed. The position of the

Raman band can be assigned according to literature or basing on theoretical calculations, isotopic substitution or symmetry considerations (Long, 2002). But usually, the last operations do require experienced spectroscopists (see par 5.1.1) . The comparison of native protein crystal and chemically modified crystal can be performed *via* difference spectra in case of off-resonance spectrum or just *via* a simple comparison of the spectra for resonance Raman (Carey, 2006).

5. Examples of Raman assistance in chemical modifications of protein crystals

Application of complementary techniques that probe different features is an added value to the understanding of the relationship between structure, function and dynamics.
Raman microscopy proved to be a valuable support to protein crystallography in all the steps of the 3D structure determination, from the preparation of the derivative crystals up to the interpretation of the electron density maps. We will first present examples of chemical composition changes (cfr 5.1), and then we will move to possible secondary (cfr. 5.2) and tertiary structure (cfr 5.3) modifications occurring upon a physico-chemical treatment.
In some cases crystallography can assist Raman spectroscopy in defining frequency assignments. In this case we speak about crystallography-assisted Raman spectroscopy.

5.1 Raman helping phase problem solution

Phase problem in crystallography can be solved for new proteins *via* multiple wavelength anomalous diffraction (MAD) or by multiple isomorphous replacement (MIR). Both these approaches usually-require a chemical modification of the protein crystals.

5.1.1 Raman detection of Se-Met incorporation into protein crystals

Se-Met derivatives are expressed for phase determination using multiwavelength anomalous dispersion (MAD) experiments (Cassetta et al., 1999). Se-Met inclusion is a widespread approach for MAD experiments since Met residues are present with an average occurrence of 1 per 59 residues (Hendrikson et al., 1990). Once crystals of a Se-Met derivative protein have been obtained, only then the absorption spectrum can be used to reveal the presence of selenium for determination of the crystal structure. Se-Met derivative crystals should be stored in a reducing environment (usually adding DTT) and diffraction experiments should be carried out using fresh crystals. It has been reported that two-week storage of Se-Met protein crystals can produce significant deterioration of the crystal diffraction power (Doublié, 1997). Since synchrotron beam-time is not always available immediately after growth of the crystals, a tool to check the Se-Met status in stored crystals is beneficial.
A Raman microscopy study was conducted on isomorphous wild-type and Se-Met crystals of the βγ-crystallin from *Geodia cydonium* (geodin) (Vergara et al., 2008). Geodin is a protein of unknown function, whose structural characterization could provide information on how homologous βγ-crystallin monomeric proteins evolved.
Table 1 summarizes the most relevant Raman bands observed in off-resonant Raman spectra for the SeMet-derivative crystals of geodin. Spectra at low frequency region (400-1200 cm^{-1}) are reported in Figures 2. Usually, the Raman spectrum of a polypeptide is subdivided into three main regions of interest: 1) the range between 870–1150 cm^{-1}, associated with the

vibrations of the backbone Cα-C and Cα-N bonds; 2) the range between 1230–1350 cm^{-1}, containing the amide III region vibrations, associated with normal modes of various combinations of the Cα-H and N-H deformations together with the Cα-C and Cα-N stretchings (Asher et al., 2001); 3) the range between 1630–1700 cm^{-1}, associated with C=O stretching modes, defined as the amide I region (Ngarize et al., 2004). Furthermore, the lower and higher regions can also be informative: i) the conformation and detection of disulphide bridges can be investigated in the low frequency (500-540 cm^{-1}) region (Kudryatsev et al., 1998); ii) hydrophobic interactions can be investigated by analysing the C-H stretching region (2800-3200 cm^{-1}) (Chourpa et al., 2006), and the S-H stretching region 2550-2600 cm^{-1} can serve as a valuable probe of local dynamics (Thomas, 1999).

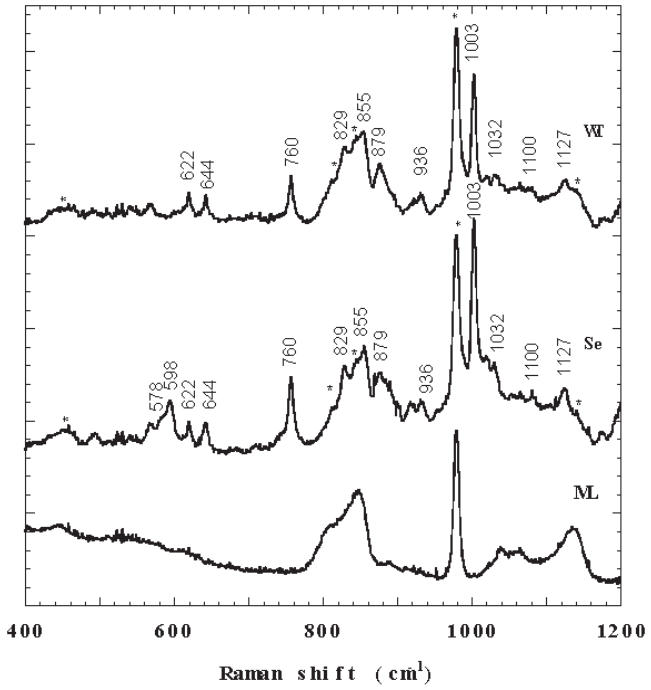

Fig. 2. Low frequency Raman spectra of the wild-type geodin crystals (WT), the Se-Met labelled crystals (Se), the mother liquor from which both kind of crystals grew up (ML). Signals attributed to the mother liquor are tagged by a star. The spectral resolution is 4 cm^{-1}. (after Vergara et al., 2008).

The Raman spectra collected on the isomorphous crystals of wild-type and Se-Met geodin crystals reveal the same secondary structure features (Amide I and III). These findings suggest that the presence of the Se-Met does not alter the structure of geodin, as observed for most of the proteins. The main difference between the two spectra (excluding the slightly different intensity of mother liquor signals) is in one narrow region at low frequency. Indeed, the bands in the 570-600 cm^{-1} region are present only in the Se-Met geodin crystal, and not in the spectra of the mother liquor or in the wild-type geodin crystal (Table 1). This

spectral feature can be confidently assigned to the C-Se stretching, in agreement with previous Raman studies on selenium-containing organic compounds (Hamada & Morishima, 1977; Paetzold et al., 1967), and on the selenomethionine aminoacid (Zainal & Wolf, 1995; Lopez et al., 1981).

Band frequency (cm^{-1})	**assignment of vibration mode**	**Primary Structure**	**Secondary structure**
	C=O stretching		**Amide I**
1668			β sheet and random coil
1650 shoulder			α-helix
1614	Ring stretching, side chain	Tyr-Phe	
1605			
1577	Ring stretching	Trp	
1548	Ring stretching	Trp	
1449	$C-H_2$ scissoring		
1400	COO^- stretching		
	N-H, C-H and CH_2 bending		**Amide III**
1318			α-helix
1245			random coil
1237			β sheet
1205	C-C stretching	Tyr-Phe	
1159			
1127	C-C stretching		
1100	C-C stretching		
1032	C-C stretching	Phe	
1003	Ring breathing	Phe	
936	C-C, skeletal stretching		
889	C-C, C-O deformations	Trp	
855	Fermi resonance doublet	Tyr	
829			
760	C-C, C-O deformations	Trp	
644	ring bending	Tyr	
622	ring bending	Phe	
598	symmetric C-Se stretching	**Se-Met**	
578 shoulder	asymmetric C-Se stretching		

Table 1. Assignment of characteristic Raman bands measured for the Se-Met derivative crystals of the crystalline-like protein from *Geodia cydonium* (geodin).

Using these assignments, SeMet Raman peaks have been observed also in the SeMet derivative of protein SOUL (Rossi et al., 2009). In these crystals, a quantitative evaluation of the relative amount of SeMet replacement was also achieved by comparative analysis.
In principle, Raman microspectra could be also used to reveal post translational modifications, such as phosphorylation, acetylation, trimethylation, ubiquitination and

glycosilation, as already done by comparing spectra of native and derivative proteins in solution (Sundararajan, et al. 2006; Brewster et al., 2011).

5.1.2 Raman detection of heavy atom derivatives

As previously stated, heavy atoms can be incorporated into protein crystals for the purposes of phasing. The simplest way to soak a heavy atom into protein crystals is to immerse the crystal straight into a drop containing the heavy atom at the final concentration for a soaking time ranging from 10 min up to several days. Different salts can be used for this purpose: successful experiences have been reported using K_2PtCl_4, $KAu(CN)_2$, K_2HgI_4, $UO_2(C_2H_3O_2)_2$, $HgCl_2$, $K_3UO_2F_5$ and para-chloromercurybenzoic sulfate (PCMBS) (Boggon & Shapiro, 2000).

During this procedure, typical question are: did actually the ion soak into the crystal? Is the time of soaking long enough for allowing the heavy atom diffusion into the crystal?

Raman microscopy can help answering these questions without waiting for a Patterson map. Reports of Raman-based direct Pt incorporation and indirect Eu^{3+} soaking are available in literature (Carpenter et al., 2007). Indeed, the Pt-Cl stretching appears at 330 cm^{-1} that can be compared to the Trp band at 760 cm^{-1}. From the time-evolution of the relative intensity I330/I760 we can follow Pt^{2+} soaking into the crystal.

Authors have recently defined a protocol to follow Hg^{2+} binding to free Cys residues (unpublished results), that is dependent on the number of Cys residues involved in the binding (1 or 2).

5.2 Raman detection of chemical modifications perturbing secondary structure

In some rare cases chemical modifications, such as pH change or Cys-Cys reduction, can significantly change even secondary structure. By taking advantage from the sensitivity of Amide I band to conformational variations, Thomas revealed a β-sheet to α-helix transition upon TCEP [tris(2-carboxyethyl)phosphine] addition to bovine insulin crystals (Zheng et al., 2004). Unfortunately, upon chemical reduction crystals do not diffract anymore, and no crystallographic counterpart is available. An analogous conformational transition occurred upon pH decrease of 5S subunit of transcarboxylate (Zheng et al., 2004), where modifications in the Amide III region (Mikhonin et al., 2006) suggested a significant modification into the crystal matrixes. Also hydration can affect deeply Amide I, and eventually secondary structure, as observed for a collagen-like polypeptide, for which Raman spectrum of the lyophilized powder showed very different Amide I frequencies when compared to single crystals (Figure 3, from Merlino at al., 2008a).

In particular, in this case, spectra of $(PPG)_{10}$ powders are characterized by three distinct well-resolved amide I bands (1638, 1655, 1690 cm^{-1}), that do not match the frequencies observed in the spectra of $(PPG)_{10}$ crystals (1629, 1645 and 1669 cm^{-1}).

The three amide I bands, and especially the well-resolved band at 1690 cm^{-1}, do not match the frequencies reported by FT-IR solution studies for the unfolded $(PPG)_{10}$ (maximum at 1633 and a shoulder at 1665 cm^{-1}) or for the unfolded polyproline (one band at 1621 cm^{-1}) (Bryan et al., 2007).

The amide I bands of $(PPG)_{10}$ crystals and powders are significantly different, not only for the intensity distribution of the crystal spectrum (depending on the orientation of the polarization of the exciting laser beam with respect to the main axes of the Raman tensor in the respective unit cell), but also for the frequency of the Raman peaks (After Merlino et al., 2008a).

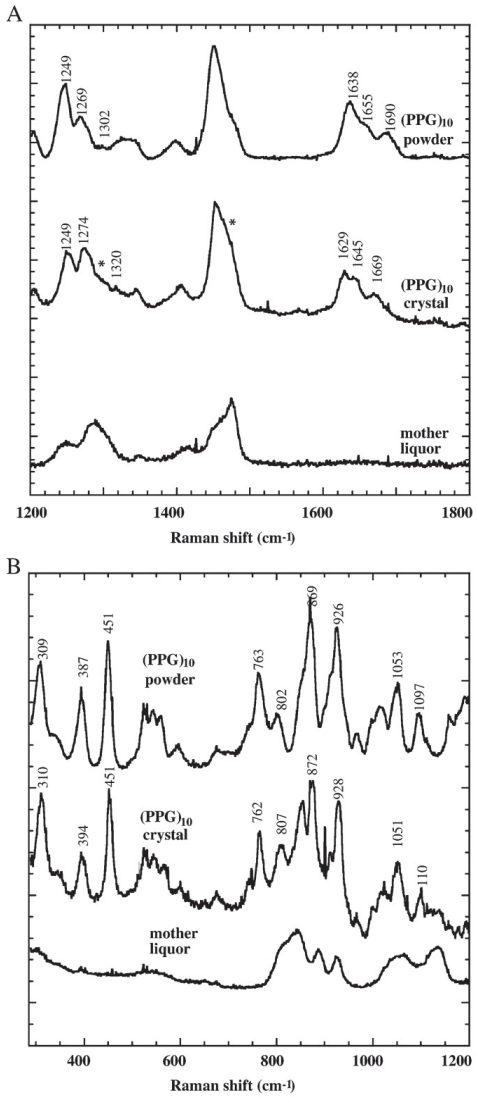

Fig. 3. Medium frequency (A) and low frequency (B) Raman spectra of $(PPG)_{10}$ powders, crystals, and mother liquor from which crystals grew up. In spectra (A) and (B) the signals attributed to the mother liquor are tagged by a star. Spectral resolution is 4 cm^{-1}. After (Merlino et al. 2008a).

5.3 Raman detection of chemical modification perturbing tertiary structure

Certainly, the most common structural modifications are related to tertiary structure. The amino-acidic modification can be followed even by off-resonance Raman spectra, whereas modification at metal center can only be detected *via* resonance Raman spectra.

5.3.1 Off-resonance Raman spectra showing tertiary structure modifications

Many Raman markers can provide information on the modified microenvironment of side chains (particularly free Cys and Tyr residues), disulfide bridges conformation or ligands entry, or metal center.

The relative intensity of Fermi resonance doublet from Tyr (I856/I830) is strictly dependent on the strength of the H-bond formed by tyrosines with the adjacent groups (1.25 exposed and 0.5 for strong H-bond donation of the OH).

Sulfidryl groups exposure of Cys residues can be investigate following the kinetics of H/D exchange *vs* temperature. Also the pKa of Cys can be extracted by titrating S-H stretching at 2550-70 cm^{-1} (mercaptoethanol 2580 cm^{-1}) compared to the envelope at 2800-3000 cm^{-1} (Thomas, 1999).

When ligand soaking is followed, difference Raman spectra can provide indication on both bound ligands and related conformation changes of the proteins. Carey reported a review of Raman-microscopy applications to follow ligand binding (Carey, 2004), and more recently he has applied this technique in kinetic crystallography to monitor time evolution of β-lactamases binding with clinical inhibitors (Carey, 2011). These spectroscopic evidences can be even used as restrains during crystallographic model refinement.

5.3.2 Resonance Raman spectra showing tertiary structure modifications

Metal centers have been well studied *via* Resonance Raman (RR) spectroscopy for hemoprotein and not-containing heme proteins. A recent example was reported for the major haemoglobin from the sub-Antarctic fish *Eleginops maclovinus*, for which a variety of coordination, spin state were observed keeping the same oxidation states (Merlino et al., 2010). In this example, Raman microscopy experiments were conducted on two different carbomonoxy crystals (called Ortho and Hexa) as well as on their ferric and deoxy forms (Figure 4).

The high-frequency region (1300–1700 cm^{-1}) of the RR spectrum includes the porphyrin in-plane vibrational modes (which are sensitive to the electron density of the macrocycle and the oxidation, coordination and spin state of the iron ion).

The deoxy forms of both Ortho and Hexa are pentacoordinated high-spin states (bands at 1355, 1548–1549, 1582 and 1602–1607 cm^{-1}). The ferric form contains a hexacoordinated low-spin hemichrome (bands at 1505, 1559, 1588 and 1640 cm^{-1}) (Merlino et al., 2011). After long laser exposure times (about 10 min), the Ortho but not the Hexa form appears to be unstable under laser irradiation, and it irreversibly converts to a hexacoordinated low-spin haemochrome state (bands at 1361, 1496 and 1587 cm^{-1}, respectively).

RR microscopy can be also used to identify anomaly in the coordination state of hemoprotein (Merlino et al., 2008b; Vergara et al., 2010). A recent and fine case is the unusual deoxy coordination found in the Antarctic fish hemoglobin from *Trematomus newnesi* (Hb1Tn) (Vergara et al., 2010). The crystal structure of deoxy form of this protein reveals distinct coordinations at the α and β hemes, and a high disorder at the EF helices of α heme, hosting the active site. Particularly, the distances His-Fe-His were unusual at the α subunits, raising doubt of hexa-coordination. The medium frequency region ruled out any contribution of bis-histidyl deoxy coordination, confirming a penta coordination. The low frequency regions clearly showed an heterogeneity in the Fe-His stretching, with a broad band attributed to the α/β structural differences in coordination (Figure 5, after Vergara et al., 2010).

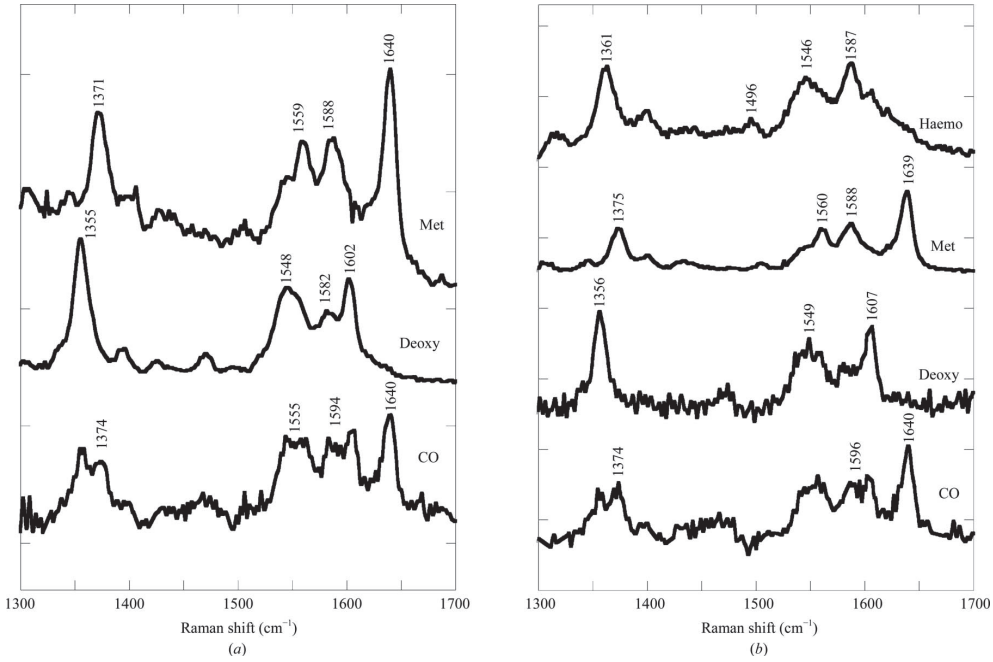

Fig. 4. Resonance Raman spectra of crystals of Hb1Em in 100 mM Tris–HCl buffer pH 8.0 at room temperature in the carbomonoxy (CO), deoxygenated (Deoxy) and ferric (Met) forms for Hexa (a) and Ortho (b) crystals. The Ortho deoxygenated form (b) converts quickly into haemochrome (Haemo) after 10 min laser exposure. Excitation wavelength, 514.5 nm; laser power at the sample 2 mW for the ferric and deoxy forms and 0.1 mW for the carbomonoxy form. All spectra were an average of at least six spectra with 2 min integration time (After Merlino et al., 2010).

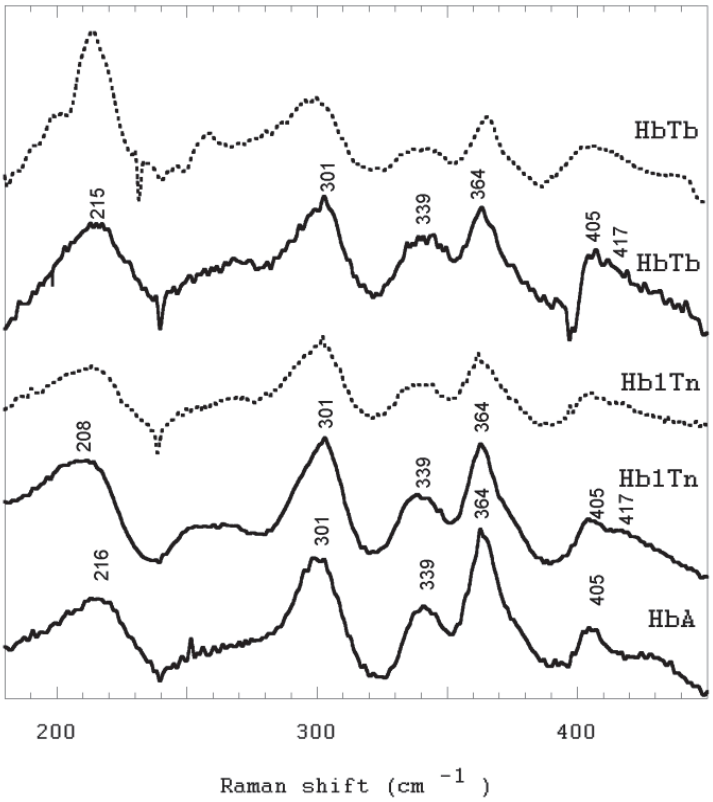

Fig. 5. Resonance Raman spectra in the low-wavenumber region of Hb1Tn (major hemoglobin of *T. newnesi*) both in solution (solid lines) and in the crystal state (dashed lines) in the deoxy state. As reference of usual coordination also HbTb (major hemoglobin of *T. bernacchii*) and human HbA are reported (After Vergara et al., 2010).

6. Raman-assisted biocrystallography to study chemical mechanisms and X-ray radiation damage

Raman assistance can go much beyond the crystal preparation and can provide additional structural information to solve some ambiguities in the electron density map interpretation. Examples include the 1) effect of X-ray damage as a function of the X-ray dose (Garman, 2010). Some examples are breakage of disulphide bonds (Carpentier et al., 2010) and Brominated-DNA photo-dissociation (McGeehan et al., 2007), and even X-ray-induced transient photobleaching in a photoactivatable green fluorescent Protein (Adam et al., 2009). Indeed, third generation synchrotrons brought back the problem of X-ray damage, even at 100 K (Garman, 2010). A complete microspectroscopic picture of the radiation damage is not yet available. The possibility to investigate the different rates of decay for different chemical groups would help crystallographers in making more stable derivative crystals. Authors are currently working on this subject in collaboration with SLS scientists. 2) X-ray induced photo-reduction that may affect metal spin and oxidation state. 3). Identification and freeze-

trapping of reaction intermediates (Carpenter et al., 2011). Bourgeois' group was pioneer in this field reporting non-resonance Raman of a trapped iron(III)-(hydro)peroxo species in crystals of superoxide reductase, a nonheme mononuclear iron enzyme that scavenges superoxide radicals (Katona et al., 2007), and further investigations came on RNA polymerase reactions as well (Carey et al., 2011). However this is out of the scope of this chapter, although it represents a formidable challenge for Raman-assisted X-ray biocrystallography.

7. Aknowledgements

This work was financially supported by PNRA.

8. References

Adam, V., Carpentier, P., Violot, S., Lelimousin, M., Darnault, C., Nienhaus, G.U. & Bourgeois, D. (2009) "Structural Basis of X-ray-Induced Transient Photobleaching in a Photoactivatable Green Fluorescent Protein" J. Am. Chem. Soc., 131, 18063

Brewster V. L., Ashton, L. & Goodacre, R. (2011) "Monitoring the glycosylation status of proteins using Raman spectroscopy" Anal. Chem., 83, 6074

Bryan, M., Brauner, J. , Anderle, G. , Flach, C. , Brodsky, B. & Mendelsohn, R. (2007) "FTIR studies of collagen model peptides: complementary experimental and simulation approaches to conformation and unfolding" J. Am. Chem. Soc., 129, 7877

Carey, P.R. (2006) "Raman crystallography and other biochemical applications of Raman microscopy, Ann. Rev. Phys. Chem., 57, 527

Carey, P R, Yuanyuan Chen, Bo Gong & Matthew Kalp, (2011) "Kinetic crystallography by Raman microscopy" Biochim. Biophys. Acta, 1814, 742

Carey, P. R. & J. Dong, (2004) "Following ligand binding and ligand reactions in proteins *via* Raman crystallography" Biochemistry, 43, 8885

Carpentier, P., Royant, A, Ohana & J. Bourgeois, D (2007) "Advances in spectroscopic methods for biological crystals. 2. Raman spectroscopy" J. Appl. Cryst., 40, 1113

Carpentier, P., Royant, A., Weik, M. & Bourgeois, D. (2010) "Raman-Assisted Crystallography Suggests a Mechanism of X-Ray-Induced Disulfide Radical Formation and Reparation" Structure, 18, 1410

Cassetta, A., Deacon, A. M., Ealick, S. E., Helliwell, J. R., & Thompson, A. W. (1999) "Development of instrumentation and methods for MAD and structural genomics at the SRS, ESRF, CHESS and Elettra facilities" J. Synchr. Rad., 6, 822

Chayen, N. (1998) "Comparative studies of protein crystallization by vapour-diffusion and microbatch techniques" Acta Cryst. D: Biol. Cryst., 54, 8

Ducruix, A. & Giegé, R. (1999) "Crystallisation of nucleic acids and proteins. A practical approach" second edition, IRL Press, Oxford.

Garman, E F. (2010) "Radiation damage in macromolecular crystallography: what is it and why should we care?"Acta Cryst. D: Biol. Cryst., 66, 339

Katona, G., Carpentier, P., Nivière, V., Amara, P., Adam, V., Ohana, J., Tsanov, N. Bourgeois, D. (2007) "Raman-assisted crystallography reveals end-on peroxide intermediates in a non-heme iron enzyme" Science, 316, 449

Kudryavtsev, A. B., Mirov, S. B., DeLucas, L. J., Nicolete, C., van der Woerd, M., Brayb, T. L. & Basiev, T. T. (1998) "Polarized Raman spectroscopic studies of tetragonal lysozyme single crystals " Acta Cryst. D: Biol. Cryst., 54, 1216

Long, D.A., (2002), "The Raman effect" John Wiley & Sons, Chichester, England

McGeehan, J. E., Carpentier, P., Royant, A., Bourgeois, D. & Ravellia, R.G.B. (2007) "X-ray radiation-induced damage in DNA monitored by online Raman" J. Synchr. Rad. 14, 99

McGeehan, J.E., Bourgeois, D., Royant, A. & Carpentier, P. (2011) "Raman-assisted crystallography of biomolecules at the synchrotron: Instrumentation, methods and applications" Biochim. Biophys. Acta, 1814, 750

McPherson, (1999) "A. Crystallization of biological macromolecules" Cold Spring Harbor Laboratory Press, New York

Merlino, A., Sica, F., Zagari, A., Mazzarella, L., Vergara, A. (2008a) "Correlation between Raman and x-ray crystallography for the collagen-model peptide $(Pro\text{-}Pro\text{-}Gly)_{10}$" Biophys. Chem. 137, 24-27

Merlino, A., Verde, C., di Prisco, G., Mazzarella, L. & Vergara, A. (2008b)"Reduction of ferric hemoglobin from Trematomus bernacchii in a partial bis-histidyl state produces a deoxy coordination even when encapsulated into the crystal phase". (2008b). Spectroscopy, Int. J. 2, 143

Merlino, A., Vitagliano, L., Howes, B., Verde, C., di Prisco, G., Smulevich, G., Sica, F. & Vergara, A. (2009) "Combined crystallographic and spectroscopic analysis of Trematomus bernacchii hemoglobin highlights analogies and differences in the peculiar oxidation pathway of Antarctic fish hemoglobins" Biopolymers, 91, 1117

Merlino, A., Vitagliano, L., Howes, B., Nicoletti, F., Balsamo, A., Giordano, D., Coppola, D., Verde, C., di Prisco, G., Smulevich, G., Mazzarella, L. & Vergara, A. (2010) "Crystallization, preliminary X-ray diffraction studies and Raman microscopy of the major haemoglobin from the sub-Antarctic fish Eleginops maclovinus in the carbomonoxy form" Acta Cryst. F: Str. Biol. Cryst., F66, 1536

Merlino, A. , Howes, B.D., di Prisco, G., Verde, C. , Smulevich, G. , Mazzarella, L. & Vergara, A. (2011) "Occurrence and formation of endogenous histidine hexacoordination in cold-adapted hemoglobins".IUBMB Life, 63, 295

Mikhonin, A. V. , Bykov, S. V. Myshakina, N. S. & Asher, S. A. (2006) "Peptide secondary structure folding reaction coordinate: correlation between UV Raman amide III frequency, ψ Ramachandran angle, and hydrogen bonding" J. Phys. Chem. B, 110, 1928

Pernice, P., Vergara, A., Sirleto, L., Aronne, A., Gagliardi, M., Fanelli, E. & Righini, G. (2011) "Large Raman gain in a stable nanocomposite based on niobiosilicate glass", J. Phys. Chem. C., 115, 17314

Reichert, T.L. Nagabhusan, M.M. Long & C.E. Bugg, (1996) "Macroscale production of crystalline interferon alpha-2B in microgravity on STS-52, In Space Technology and Application International Forum (STAIF-96)", (El-Genk, M.S., ed.), American Institute of Physics, Woodbury, N.Y., 361, 139

Richards, J.P., M.P. Stickelmmeyer, B.H. Frank, S. Pye, M. Barbeau, J. Radziuk, G.D. Smith & M.R. Defelippis, (1999) "Preparation of a microcrystalline suspension formulation of Lys(B28)Pro(B29)-human insulin with ultralente properties" Pharm. Sci., 88, 861

Rossi, B., G. Mariotto, E. Ambrosi & H. L. Monaco (2009) "Raman scattering investigation of selenomethionine replacement in protein SOUL crystals" J. Raman Spectroscopy, 40, 1844.

Smulevich, G. & Spiro, T. G. (1993) "Single-crystal micro-Raman spectroscopy" Meth. Enzymol., 226, 397

Stoner-Ma, D., Skinner, J.M., Schneider, D.K., Cowan,M., Sweet, R.M. & Oliver, A.M., (2011) "Single-crystal Raman spectroscopy and X-ray crystallography at beamline X26-C of the NSLS" J. Synchr. Rad., 18, 37

Sundararajan, N. Mao, D. Q., Chan, S., Koo, T. W., Su, X., Sun, L., Zhang, J.W., Sung, K. B., Yamakawa, M., Gafken, P. R., Randolph, T., McLerran, D., Feng, Z. D., Berlin, A. A. & Roth, M. B. (2006) "Ultrasensitive detection and characterization of posttranslational modifications using Surface-Enhanced Raman Spectroscopy" Anal. Chem., 78, 3543

Tardieu, A. (1998) "Alpha-crystallin quaternary structure and interactive properties control eye lens transparency" Int. J. Biol. Macromol., 22, 211

Thomas, G. J. J. (1999) "Raman spectroscopy of protein and nucleic acid assemblies" Ann. Rev. Biophys. Biomol. Struct., 28, 1

Tsuboi, M., Benevides, J.M. &. Thomas, G.J. Jr. (2007) "The Complex of Ethidium Bromide with Genomic DNA: Structure Analysis by Polarized Raman Spectroscopy" Biophys. J., 92 928

Vergara, A., Lorber, B. Zagari, A., Giegé, R. (2003) "Physical aspects of protein crystal growth investigated with the Advanced Protein Crystallization Facility in reduced gravity environments" Acta Cryst. D: Biol. Cryst., 59, 2

Vergara, A., Merlino, A., Pizzo, E., D'Alessio, G. & Mazzarella, L. (2008) "A novel method for detection of seleno-methionine incorporation in protein crystals *via* Raman microscopy" Acta Cryst. D., D64, 167

Vergara, A., Castagnolo, D., Carotenuto, L., Vitagliano, L., Berisio, R., Sorrentino, G., García-Ruiz, J.-M. , Zagari, A. (2009)"Phase behavior and crystallogenesis under counter-diffusion conditions of the collagen-model peptide $(Pro\text{-}Pro\text{-}Gly)_{10}$" J. Cryst. Growth, 311, 304

Vergara, A., Vitagliano, L., Marino, K., Merlino, A., Sica, F., Verde, C., di Prisco G. Mazzarella, L. (2010) "An order-disorder transition plays a role in switching off the Root effect in fish hemoglobins" J. Biol. Chem., 285, 32568

Vitagliano, L., Vergara A., Bonomi, G., Merlino, A., Smulevich, G., Howes, B., di Prisco, G., Verde, C. & L. Mazzarella, (2008) "Spectroscopic and crystallographic analysis of a tetrameric hemoglobin oxidation pathway reveals features of an intermediate R/T state" J. Am. Chem. Soc., 130, 10527

Zheng, R., Zheng, X., Dong, J. & Carey, P.R. (2004) "Proteins can convert to β-sheet in single crystals" Prot. Sci., 13, 1288

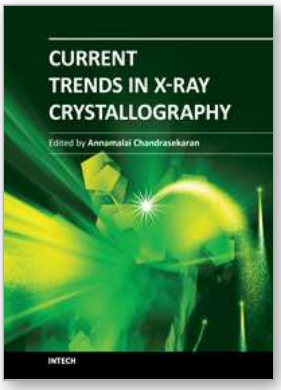

Current Trends in X-Ray Crystallography

Edited by Dr. Annamalai Chandrasekaran

ISBN 978-953-307-754-3
Hard cover, 436 pages
Publisher InTech
Published online 16, December, 2011
Published in print edition December, 2011

This book on X-ray Crystallography is a compilation of current trends in the use of X-ray crystallography and related structural determination methods in various fields. The methods covered here include single crystal small-molecule X-ray crystallography, macromolecular (protein) single crystal X-ray crystallography, and scattering and spectroscopic complimentary methods. The fields range from simple organic compounds, metal complexes to proteins, and also cover the meta-analyses of the database for weak interactions.

How to reference

In order to correctly reference this scholarly work, feel free to copy and paste the following:

Antonello Merlino, Filomena Sica and Alessandro Vergara (2011). Monitoring Preparation of Derivative Protein Crystals via Raman Microscopy, Current Trends in X-Ray Crystallography, Dr. Annamalai Chandrasekaran (Ed.), ISBN: 978-953-307-754-3, InTech, Available from: http://www.intechopen.com/books/current-trends-in-x-ray-crystallography/monitoring-preparation-of-derivative-protein-crystals-via-raman-microscopy

INTECH
open science | open minds

InTech Europe
University Campus STeP Ri
Slavka Krautzeka 83/A
51000 Rijeka, Croatia
Phone: +385 (51) 770 447
Fax: +385 (51) 686 166
www.intechopen.com

InTech China
Unit 405, Office Block, Hotel Equatorial Shanghai
No.65, Yan An Road (West), Shanghai, 200040, China
中国上海市延安西路65号上海国际贵都大饭店办公楼405单元
Phone: +86-21-62489820
Fax: +86-21-62489821